Journal of Colloid and Interface Science 469 (2016) 257–262

Contents lists available at ScienceDirect

Journal of Colloid and Interface Science

journal homepage: www.elsevier.com/locate/jcis

Short Communication

Electrochemical behavior of chemically synthesized selenium thin film

A.M. Patil [a], V.S. Kumbhar [a], N.R. Chodankar [a], A.C. Lokhande [b], C.D. Lokhande [a,*]

[a] Thin Film Physics Laboratory, Department of Physics, Shivaji University, Kolhapur, M.S. 416 004, India
[b] Department of Materials Science and Engineering, Chonnam National University, 500-757, South Korea

GRAPHICAL ABSTRACT

(a) Image shows surface morphology of selenium thin film with unequal nanoparticles. Inset AFM figure supports SEM analysis. The inside Ragone plot displays supercapacitive behavior of selenium electrode material, and (b) the formation of selenium thin film on stainless steel substrate as nucleation, aggregation, coalescence and grouth of particles.

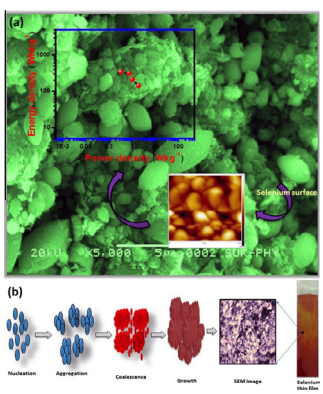

ARTICLE INFO

Article history:
Received 11 December 2015
Revised 7 February 2016
Accepted 9 February 2016
Available online 10 February 2016

Keywords:
Selenium
Thin film
Chemical bath deposition
Electrochemical properties

ABSTRACT

The facile and low cost simple chemical bath deposition (CBD) method is employed to synthesize red colored selenium thin films. These selenium films are characterized for structural, morphological, topographical and wettability studies. The X-ray diffraction (XRD) pattern showed the crystalline nature of selenium thin film with hexagonal crystal structure. The scanning electron microscopy (SEM) study displays selenium nanoparticles ranging from 20 to 475 nm. A specific surface area of 30.5 $m^2 g^{-1}$ is observed for selenium nanoparticles. The selenium nanoparticles hold mesopores in the range of 1.39 nm, taking benefits of the good physicochemical stability and excellent porosity. Subsequently, the electrochemical properties of selenium thin films are deliberated by cyclic voltammetry (CV), galvanostatic charge–discharge and electrochemical impedance spectroscopy (EIS) techniques. The selenium thin film shows specific capacitance (C_s) of 21.98 F g^{-1} with 91% electrochemical stability.

1. Introduction

During past few years, a significant interest in selenium has increased appreciably owing to number of applications such as modern electronics, optoelectronics, new generation sensors and

* Corresponding author.
E-mail address: l_chandrakant@yahoo.com (C.D. Lokhande).

http://dx.doi.org/10.1016/j.jcis.2016.02.030
0021-9797/

photovoltaic cells [1,2]. The unique photoelectric and semiconducting properties of selenium find applications in rectifiers, photocells, switching electronic devices, memory devices and X-ray photoconductors [3]. Elemental selenium is almost present in environmental and biological materials. Selenium has several oxidation states such as Se^{2-}, Se^{0}, Se^{4+} and Se^{6+} and exhibits different structures namely amorphous, trigonal (hexagonal), α-monoclinic and β-monoclinic. The structure of selenium consists of chains (Se_n) and rings (Se_8) [4]. Now days, sulfur is replaced by selenium in Li–S batteries, because of the insulating nature of sulfur and dissolution of reductive polysulfide in organic electrolytes during cycling which moderately affect the performance of Li–S batteries [5]. More importantly, the higher electrical conductivity (~20 times greater than sulfur) is desired for lithium ion batteries [6]. The selenium is also used as a dopant in lead acid batteries, where it increases the corrosion resistance and discharge capacities [7]. Even all these features, no reports are available on the electrochemical supercapacitive features of selenium.

In the past, selenium thin films have been prepared by various physical as well as chemical deposition methods [8–11]. In present work, selenium thin films are synthesized by chemical bath deposition (CBD) method, which is binder-free, surfactant-less, low cost and simple as compared to other physical and chemical deposition methods. Subsequently, the electrochemical properties of selenium thin films are studied.

2. Experimental

For deposition of selenium thin film, the stock solution of 0.0125 M Na_2SeSO_3 was prepared by dissolving selenium powder in aqueous solution of 0.0125 M Na_2SO_3 with pH~10.2 (±0.1). The 0.0125 M Na_2SeSO_3 solution was acidified at room temperature (300 K) by adding acetic acid and pH was maintained at 4.4 (±0.1). The well cleaned stainless steel (SS) substrate was dipped in acidified solution of Na_2SeSO_3. After 5 h, red colored selenium thin film was deposited on SS substrate. The substrate was taken out from the bath, washed several times in double distilled water (DDW) and dried at room temperature (300 K).

The selenium thin film structure was characterized by XRD technique using a Bruker AXS D8 advanced Model with copper radiation (K_α of wavelength = 1.54 Å). The phase confirmation was accomplished by Raman spectrometer (Bruker MultiRAM, Germany). Surface morphological investigation was done by scanning electron microscope (SEM), (JEOL-JSM 6360) and atomic force microscopy (AFM) Model-INNOVA 1B3BE units. The energy dispersive X-ray analysis (EDAX) was collected by JEOL-JSM 6360 unit. The contact angle measurement was carried out by Rame-Hart equipment with CCD camera. The specific surface area of a selenium material was calculated by Brunauer, Emmett and Teller (BET) model Quantachrome Instruments v11.02. The thickness of selenium thin film was measured using XP-1 Stylus surface profiler with laser calibration. Electrochemical properties of selenium thin films were executed by automatic battery cycler unit (WBCS3000) and EIS analysis was carried out using electrochemical workstation (ZIVE SP5) in 1 M Na_2SO_4 electrolyte.

3. Results and discussion

The CBD route involves several steps for film formation such as nucleation, aggregation, coalescence and growth of particles. The nucleation conducts heterogeneous reaction on the film surface. The cluster of molecule inaugurated undergoes rapid decomposition with combination of particles to grow film up to certain thickness [12]. With addition of acetic acid in precursor solution (0.0125 M Na_2SeSO_3), the precipitate starts and solution becomes saturated. The proposed reaction mechanism is as follows,

$$Na_2SO_3 + Se \rightarrow Na_2SeSO_3 \quad (1)$$

$$Na_2SeSO_3 + 2CH_3COOH \leftrightarrow Se\downarrow + 2CH_3COONa + SO_2\uparrow + H_2O \quad (2)$$

Fig. 1(A) shows XRD pattern of selenium thin film. The diffraction planes corresponding to the (1 0 0), (1 0 1) and (1 1 0) planes of hexagonal structure for selenium having lattice parameters of a = 4.3639 Å and c = 4.9595 Å [JCPDS card No. 65-1876] are observed. The peaks of SS substrate are denoted by asterisk (∗). The crystallite size of selenium is calculated as 29.8 nm by full width at half maxima (FWHM) for high intense peak (1 0 1) using Scherrer formula [13]. The vibrational, rotational and other low-frequency modes in a selenium material were detected by Raman spectroscopy technique. The high intense peaks observed at frequencies of 236 and 254 cm^{-1} are in well agreement with formation of selenium (Se_8 rings) (Fig. 1(B)). The resonance peak observed at 236 cm^{-1} is a characteristic stretching mode (A_1), which represents chain-like structure existing in hexagonal selenium [14]. Inset figure confirms that selenium surface is a hydrophilic, as water contact angle is 47°. Fig. 1(C and D) shows SEM images of selenium thin film at magnifications of 2000× and 5000×. At low magnification, selenium surface is covered with nanoparticle like grains. At higher magnification, interconnection of nanoparticles distributed throughout film surface is observed. Fig. 1(E) depicts EDAX spectrum of selenium thin film. High intense spectrum of selenium confirms selenium deposition on SS substrate. The inset of figure shows atomic (96.64%) and weight (99.38%) percentages of selenium. Fig. 1(F) shows 3-D AFM image of selenium film surface with elliptical shaped nanoparticles at scan range of 10 μm, which supports the SEM analysis. The average particle size and roughness are calculated to be 120 nm and 20.7 nm, respectively. The nanoparticles consist of cluster of atoms having different size ranging from 100 to 500 nm. The thickness of selenium thin film on SS substrate is about 585.3 nm for deposition time of 5 h. The thickness of selenium thin film on SS substrate can be adjusted by varying deposition time. Also, the mass of selenium material on SS substrate of area 1 × 1 cm^2 is about 0.33 mg. Such a small amount of selenium contribute in electrochemical reaction of electrode–electrolyte. The surface cross sectional resistance of selenium thin film on SS substrate is measured to be 0.67 Ω for 1 × 1 cm^2 area.

The nitrogen adsorption–desorption measurements are used to study the porosity and textural properties of selenium nanoparticles. The nitrogen adsorption–desorption isotherm is represented in Fig. 2(A). The curve expose type IV isotherm attended by H_3 type hysteresis loop in the IUPAC classification, representing the existence of mesopores with specific surface areas of 30.5 $m^2 g^{-1}$ [15]. The type H_3 hysteresis loop is related with capillary condensation happening in nanoparticle shaped mesopores, which may create from the collection of nanoparticles of selenium thin film. The pore size distribution of the fine interconnected nanoparticles was fitted via Barrett–Joyner–Halenda (BJH) model (see Fig. 2(B)). The selenium nanoparticles show higher mesoporosity and exhibits relatively high intense peak at around 1.39 nm. It can provide low-resistant trails for the ions through the porous structure, as well as a smaller diffusion path owing to the systematic mesoporous channels. The plots confirm major volume of pores in the mesopore range [16]. Pore sizes are larger than the size of the electrolyte ions used in the energy storage devices and will allow fast flow of the electrolyte ions into selenium electrode. The better specific surface area and porosity enhance the intercalation/deintercalation reaction between electrode and electrolyte. The superior surface area provides more active sides in electrochemical